1 Introduction into the spectroscopy and interactions of metal and metal cation complexes

1.1 Introduction into interactions within metal complexes

Metals and their interactions with ligands are ubiquitous in chemistry. They play a vital role in many biological processes, in addition to being pivotal in catalyzing many industrial chemical processes.[1,2] Understanding the fundamental interactions present in these metal complexes is essential in further developing our knowledge of the many reactions and processes in which these interactions play a key part.

In many cases the metal and ligand are not bound through a chemical interaction in which electron density is exchanged as in an ionic bond or shared as is the case of a covalent covalent bond, but instead through physical interactions such as electrostatic, inductive and dispersive interactions.

Electrostatic interactions are the interaction between pairs of ions and molecules in which there is a permanent charge, dipole or multipole. Inductive interactions are the result of the interaction between either an ion, or molecule with a permanent dipole or multipole, with a non-polar molecule in which a dipole or multipole has been induced by the interacting partner. Dispersive or van der Waals interactions occur in non-polar molecules where a random dipole in one of the interacting partners induces a dipole in the other. Although the strength of these interactions is dependent on the actual interacting partners, for example the charge on the ion, the size of the dipole in a polar molecule or the polarizability of a non-polar molecule, each general pairing is inversely dependent on the internuclear separation, R. For example ion/permanent dipole interactions have an R^{-2} dependance, whilst a random dipole/induced dipole interaction has a dependence of R^{-6}.

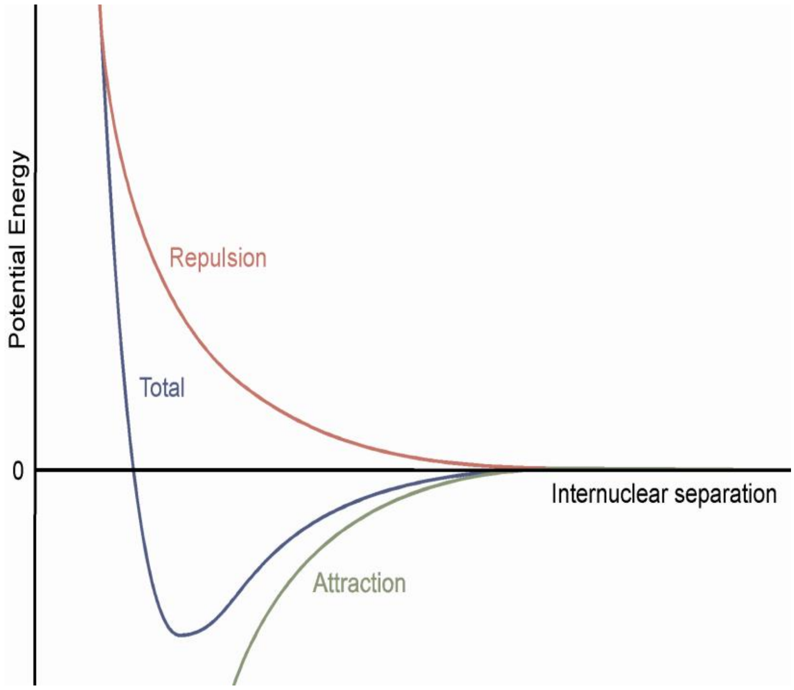

Figure 1.1. The general form of a potential energy curve.

The interactions described above are attractive interactions, however, there are a number of repulsive interactions comprising nuclear, electronic and Pauli (exclusion principle) repulsions that need to be considered in order that the overall interaction with respect to R between the interacting partners, known as the potential energy curve, can be determined. A typical potential energy curve is shown in

Figure 1.1. As can be seen, at long range the attractive interactions dominate, however, as *R* decreases it is the repulsive forces become more prominent.

This thesis presents work on metal-ligand complexes bound in the most part by physical interactions. In the Chapters focusing on Au-RG complexes the fundamental interactions between metals and ligands are investigated for the interaction of two "inert" species, where this could be expected to be the ideal system to study physical interactions.

The interaction of metals and metal cations, introduced through the ablation of meteorites, with atmospheric ligands in the mesosphere lower thermosphere (MLT) region of the atmosphere is also considered. The results of high level *ab initio* calculations, that enable the ion-molecule chemistry of calcium and magnesium to be modelled, are presented. It is hoped that this will lead to a better understanding of the sensitive mesospheric region of the atmosphere, in particular the natural phenomena of neutral sporadic metal layers that occur in region.

1.2 Au-RG complexes

1.2.1 Interest in Au-RG complexes

In recent years there has been an increasing interest in the Au-rare gas (RG) complexes.[3,4,5,6,7,8] Interest in these complexes arises as they ought to be relatively simple systems ideal for the study of fundamental chemical and physical interactions of metals.[1,2,3,4,5,6,7,8,9,10,11,12,13,14] The comparison of these Au-RG complexes to studies of the other CM–RG complexes,[8,9,10,11,15,16,17] in which CM is a coinage metal (Cu, Ag, Au), also allows relativistic effects and the lanthanide contraction to be investigated.

Recently, a number of studies[9,14,18] have concentrated on the fundamental chemical question of what actually constitutes a chemical bond. In these studies a number of metal cation (M^+) - RG complexes were investigated to determine whether the interactions between the moieties were entirely physical or whether there are covalent contributions to the bonding present in these species. In the majority of cases, it was shown by Breckenridge and co-workers[9,19,20] that when all the physical terms out to $1/R^8$ were included, the dissociation energies of the M^+-RG complexes could be adequately explained without the need to invoke extra covalent effects. However, a number of exceptions were found[9] one of which, in agreement with comments made by Pyykkő and co-workers,[21,22] was the strongly bound Au^+-Xe complex. Further studies[14] also found that purely physical interactions were not entirely sufficient to explain the bond energies of the Au^+-Ar and Au^+-Kr species. It was commented[14] that it would be desirable to have experimental bond lengths and dissociation energies, D_0'', for the Au^+-RG series to which the high level *ab initio* values could be compared. One way to investigate these Au^+-RG complexes is through two-colour high-resolution photoelectron spectroscopy, in which a logical first step would be the excitation to an intermediate electronic state. As such, the characterization of excited states in the Au-RG complexes would be important to enable the study of these cationic species and is part of the impetus for the work detailed in this thesis.

1.2.2 Electronic states of interest in the Au-RG complexes

The states that have been investigated within this thesis are the molecular states corresponding to the strong ${}^2P_J \leftarrow {}^2S$ (where $J = {}^1/_2, {}^3/_2$) atomic transition on Au. As can be seen in Figure 1.2 there are three diatomic states that arise from the interaction between the Au ${}^2P_J$ states with the RG atom: the $D^2\Pi_{1/2}$ state correlating to the Au(${}^2P_{1/2}$) + RG(${}^1S_0$) asymptote and the $D^2\Pi_{3/2}$ and $E^2\Sigma_{1/2}^+$ states correlating to the Au(${}^2P_{3/2}$) + RG(${}^1S_0$) asymptote. The electronic ground state of the Au-RG complex, $X^2\Sigma_{1/2}^+$, is formed from the interaction between the Au and RG atoms in their ${}^2S_{1/2}$ and ${}^1S_0$ respective atomic ground states.

As can be seen from Figure 1.2 there are a number of states that lie in between the $X^2\Sigma_{1/2}^+$ ground state and the two $D^2\Pi_\Omega$ (where $\Omega = {}^1/_2, {}^3/_2$) states, which arise from the Au(${}^2D_J$) + RG(${}^1S_0$) asymptotes. Although these states were not spectroscopically investigated they are potentially important in the spectroscopy of the states arising from the Au (${}^2P_J$) + RG (${}^1S_0$) asymptotes and hence, as maybe seen in later Chapters, were considered in *ab initio* calculations. It is worth noting that the position of the ${}^2D_J$ states relative to the ${}^2S_{1/2}$ varies as you go down the coinage metals series.[23,24,25] The relative position and ordering of the ${}^2D_J$ states in Cu is similar to those in Au, shown on the right-hand side of Figure 1.2, with the $^2D_{5/2}$ state 11202.6 cm^{-1} and 9161.2 cm^{-1} above the $^2S_{1/2}$ state in Cu[23] and Au[25] respectively. However, in Ag[24] these ^2D_J states are considerably higher in energy with the $^2D_{5/2}$ state located 30242.3 cm^{-1} above the $^2S_{1/2}$ state. In fact in atomic Ag the $^2D_{5/2}$ is located above the $^2P_{1/2}$ state.[24] The ordering observed is a result of increasing relativistic stabilization with increasing atomic number of the CM, and the presence of the lanthanide contraction in Au but not Ag.

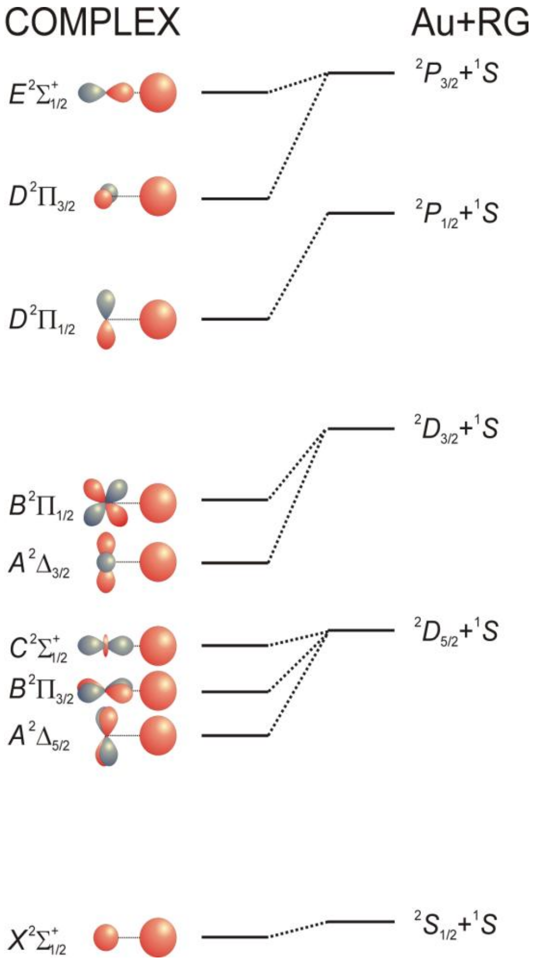

Figure 1.2. Schematic diagram showing the relationship between the atomic states, on the right-hand side of the figure with the molecular ones, on the left-hand side. Note that for the *A*, *B*, and *C* states the large doubly occupied (Au) 6*s* orbital surrounding the much smaller, singly occupied (Au) 5*d* orbitals has been omitted for the sake of clarity.

Although not shown on the schematic, the next lowest molecular state arises from Au ($^4P_{5/2}$) + Xe ($^1S_0$) asymptote. The $^4P_{5/2}$ atomic state is at 42163.5 cm^{-1} which is only 988.9 cm^{-1} above that of the $^2P_{3/2}$ state. Owing this close proximity, the possibility for interactions involving the states arising from the Au($^2P_{5/2}$) + Xe($^1S_0$) asymptote need to be kept in mind.

1.2.3 Previous investigations of the CM-RG complexes

The CM-RG complexes have over the last few years attracted much attention. However, for the Au-RG complexes the only experimental work published in the open literature is on the Au-Ar complex,[3] with a further study on the Au-Kr complex[4] being presented in a thesis chapter. Both of these studies were carried out using resonance enhanced multiphoton ionization (REMPI) and each reported spectra obtained for the $D^2\Pi_{1/2}$ and $D^2\Pi_{3/2}$ states.

A general observation from these previous studies[3,4] was that the observed excited states, $D^2\Pi_{1/2}$ and $D^2\Pi_{3/2}$, were much more strongly bound than the corresponding $X^2\Sigma_{1/2}^+$ state, evinced by the spectral red shift of the Au-RG complex origin transition relative to the corresponding transition in the uncomplexed metal. This difference in bonding was attributed to the spatial orientation of the unpaired $6p\pi$ electron density in the $D^2\Pi$ states being located off the internuclear axis in comparison to that of the unpaired $6s\sigma$ electron in the ground state (Figure 1.2). The lowering of the electron density from the internuclear axis leads to a reduction in the electron repulsion with the RG atoms in addition to deshielding the cationic Au core.

Conversely, the $E^2\Sigma_{1/2}^+$ state is expected to be very weakly bound owing to the onset of repulsion between the axial $6p\sigma$ electron and the electrons of the RG atom at even moderate R, resulting in the non-observance of this state in any previous CM-RG study. From comparison between the two previous studies it can be seen that, as expected the interaction between the heavier more polarisable Kr with the Au atom is stronger than that of Ar each in any of the $X^2\Sigma_{1/2}^+$ state or the excited $D^2\Pi_{1/2}$ and $D^2\Pi_{3/2}$ states. Further information on these previous experimental studies is given within the relevant Chapters of this thesis: Chapter 3 for Au-Ar and Chapter 4 for Au-Kr. Three recent theoretical studies on Au-He,[6,8] Au-Ne,[8] Au-Ar[8] and Au-Xe[7] are also commented on in later Chapters where relevant.

As mentioned above, there has been a number of studies on the other CM-RG species. Experimentally, the Cu-Kr,[10] and Ag-Ar/Kr/Xe[9] complexes have been investigated using resonance enhanced multiphoton ionization (REMPI) spectroscopy with Ag-Ar[11] having been additionally studied using laser induced fluorescence, whilst Cu-He,[6] Cu-Ne,[8] Cu-Ar,[8,15,16] Cu-Kr,[15] Ag-He,[6,8] Ag-Ne,[8] Ag-Ar[8] and Ag-Xe[17] have been studied theoretically.

The experimental studies again, as in the case of the Au-RG complexes, concentrated on the $^2\Pi_\Omega \leftarrow X^2\Sigma_{1/2}^+$ transitions (although in Ag-RG studies states arising from the Ag(^2D_J) + RG($^1S_0$) asymptotes were also observed) with similar observations regarding the increased binding energies of the $^2\Pi_\Omega$ states to that of the $X^2\Sigma_{1/2}^+$ state owing, as mentioned above, to a difference in the spatial orientations of the electron density in these states. As in the Au-RG complexes, the $^2\Sigma_{1/2}^+$ state arising from the CM($^2P_{3/2}$) + RG($^1S_0$) asymptotes was not observed. In the study of the Ag-RG complexes, as expected, the binding energy was observed to increase on moving to heavier, and hence more polarizable, rare gases both in the ground and excited states.[9] It was noted, however, that the trend in dissociation energies did not follow the RG polarizabilities, with Ag-Xe complex being more bound than expected.[9] It should be noted that the theoretical value obtained by Li *et al.*[17] for Ag-Xe was even higher than that obtained experimentally[9] although it is suspected that this theoretical value is in error.[26]

A more surprising result was found for the experimentally-determined ground state binding energy of Cu-Kr[10] (408 cm^{-1}), which was observed to be three times greater than that of Ag-Kr[9] (138 cm^{-1}). The observation is surprising as the polarizability of Ag (7.2×10^{-24} cm^3) is greater than that of Cu (6.1×10^{-24} cm^3). The explanation given for this result was the possibility that significant *sd* hybridization would occur in Cu-Kr but not in Ag-Kr, owing to low lying ^2D states in Cu.[10,3] As stated earlier, owing to relativistic effects and the lanthanide contraction, Au also has low lying ^2D states, thus it would be expected that Au-Kr ground state would also be considerably bound. However, this is contrary to the findings from the subsequent studies on the Au-Kr complex by Wallimann[4] and the present work indicating that the experimentally derived value for the Cu-Kr $X^2\Sigma_{1/2}^+$ state is in need of verification. This view would be in-line with the much smaller Cu-Kr D_e'' value of 149.3cm^{-1} obtained theoretically by Shen and

BelBruno[15] employing the CCSD(T) method. For the Cu-Ar complex the D_e'' value of 67.6 cm^{-1} obtained by Shen and BelBruno[15] again using the CCSD(T) method was in good agreement with the value of 62.1 cm^{-1} obtained by Bera *et al.*[16] using the CCSD(T) method combined with a Lennard-Jones potential analysis, giving confidence in the calculated Cu-Kr result. Other theoretical CM-RG results will be commented on in later Chapters where relevant.

1.2.4 Present study on Au-RG complexes

The work presented in the following Chapters uses REMPI to investigate the molecular states of the Au-RG series in the vicinity of the $^2P_J \leftarrow {}^2S_{1/2}$ atomic transitions. To aid the interpretation of this spectroscopy a number of high-level *ab initio* calculations have been performed that include the potential interactions that can occur between the various states outlined above in the Au-RG complexes.

From this work, spectroscopic constants in both the ground and excited states can be determined and hence trends down the RG series observed. Comparison of these results to those of other CM-RG will allow the effect of relativistic and lanthanide contractions to be explored. The characterization of vibrational levels in the excited states will be valuable in further studies on Au$^+$-RG complexes.

1.3 Metal and metal cation complexes important in the chemistry of the MLT region of the atmosphere

1.3.1 Introduction to metals in the MLT region of the atmosphere

The MLT region of the Earth's atmosphere, which lies between 80-110 km above the surface, is unique in that it is the only part of the Earth's atmosphere in which metals exist in the free atomic state. It is accepted that the primary source of metallic species in this region is the ablation of meteorites as they enter the Earth's atmosphere,[27] so it might quite naturally be expected that that the abundances of metals would be in a similar ratio to that found in chondritic meteorites. However, this does not appear to be the case: observed calcium levels, for instance, are reduced from these nominal values by factors of between 120-360.[28] Evidence suggests that this huge difference can be attributed to a differential ablation process in the upper atmosphere, which initially proceeds with evaporation of the relatively volatile elements, such as K and Na, whilst refractory elements such as Ca evaporate later.[29] A fraction of these ablated metals (M) are ionized by hyperthermal collisions with atmospheric molecules and produce M^+. M^+ ions can also be produced by photoionization (reaction 1.1) and charge transfer reactions with the ambient NO^+ and O_2^+ ions (reactions 1.2 and 1.3) that are dominant in the lower E region of the Earth's atmosphere.

$$M + h\nu \rightarrow M^+ + e^- \qquad (1.1)$$

$$M + NO^+ \rightarrow M^+ + NO \qquad (1.2)$$

$$M + O_2^+ \rightarrow M^+ + O_2 \qquad (1.3)$$

The presence of a layer of free metal atoms in the atmosphere has been accepted since 1929 with the observation of sodium fluorescence lines in the twilight-airglow.[30] Other metals such as Fe and K have been observed by the same technique. The current method for the detection of metal layers in the upper atmosphere is by the use of LIDAR (LIght Detection And Ranging), which can be thought of as a "laser radar". Using LIDAR, it is possible to use metal atoms as tracers of atmospheric dynamics, such as tides, gravity waves[31,32] and temperature,[33,34] allowing an improved understanding of the MLT region. Essential to the interpretation of results obtained by LIDAR is a comprehensive knowledge of the chemistry of these metal layers. Such knowledge is also important in other fields of study, as metal layers have a significant impact on radio communications, both facilitating over-the-horizon high-frequency communication and obscuring space-to-ground communications, depending on time of day and transmission frequency. [35] It has also been speculated that metal layers could act as a sensitive indicator to climate change in the MLT region either directly or through their relationship with noctilucent clouds.[35,36]

An interesting phenomenon of the MLT region is *sporadic* or *sudden neutral metal layers*, M_s, which are thin layers of metal atoms 1-3 km thick and 100s of km long that appear suddenly over a matter of minutes, last for several hours, and then disappear rapidly. These layers appear between altitudes of 90-105 km and are defined by an abrupt increase in the metal density over the level of the background mesospheric metal layers, sometimes by over an order of magnitude.[37] The occurrence of this phenomenon is believed to be the result of the neutralization of metallic ions in sporadic E plasma layers (E_s), which show a high correlation in space and time with M_s.[38,39,40,41,42,43] E_s are thin layers of metallic ions that are similarly only around 1-3 km thick and observed at altitudes between 90-140 km. They are often associated with meteor showers, which provide a large input of metallic ions, and auroral activity, where electron precipitation causes enhanced ionization of the MLT region. The E_s layers are a result of these metallic ions being concentrated into layers at null points of wind shears owing to the ions experiencing electrostatic and magnetic forces when undergoing horizontal wind transport across the Earth's magnetic field lines.[35,44] Whilst the neutralisation of the metal ions in this region can occur through radiative recombination with electrons (reaction 1.4), in all cases it is found that this mechanism is very inefficient,[45] with the first step likely to be the formation of weakly bound molecular ions by reaction of M^+ with O_3 (reaction 1.5) or by recombination of M^+ with X (=N_2, O_2, CO_2 or H_2O) in the presence of a third body, A (reaction 1.6).

$$M^+ + e^- \rightarrow M + h\nu \tag{1.4}$$

$$M^+ + O_3 \rightarrow MO^+ + O_2 \tag{1.5}$$

$$M^+ + X + A \rightarrow M^+{-}X + A \qquad (1.6)$$

This cluster ion can then form an energized diligand intermediate ($X{-}M^+{-}Y^*$) which can then decompose to yield either M^+-X +Y or $M^+{-}Y + X$ (reaction 1.7a), or, if the pressure is high enough, be stabilized by a third body A (reaction 1.7b). Stabilization of the diligand intermediate by A may also occur if Y = X (reaction 1.8), and this can initiate the build up of a cluster. In particular, for the case X = H_2O, ion hydrates have been postulated as ice nuclei for noctilucent clouds.[46]

$$M^+{-}X + Y \rightarrow X{-}M^+{-}Y^* \rightarrow M^+{-}Y + X \qquad (1.7a)$$

$$\rightarrow X\text{-}M^+{-}Y^* + A \rightarrow X{-}M^+{-}Y + A \qquad (1.7b)$$

$$M^+{-}X + X + A \rightarrow X{-}M^+{-}X + A \qquad (1.8)$$

Neutralization occurs through the dissociative recombination of the $M^+{-}Y$ complex with electrons to form the neutral atomic metal[47] (reaction 1.9). This is a more efficient process than radiative recombination because of the departing fragments being able to take up the substantial energy released as translational energy and internal excitation.

$$M^+{-}Y + e^- \rightarrow M + Y \qquad (1.9)$$

As well as dissociative recombination, these metallic cluster ions can also be converted back to M^+, e.g. the attack on the $M^+{-}Y$ ion by atomic O (reactions 1.10 and 1.11), thereby slowing down the rate of neutralisation of M^+.

$$M^+–Y + O \rightarrow MO^+ + Y \tag{1.10}$$

$$MO^+ + O \rightarrow M^+ + O_2 \tag{1.11}$$

The important reactions in the MLT region of the Earth's atmosphere are summarized in Figure 1.3, although it should be noted that this diagram is most appropriate when M = Mg^+ and Ca^+ for which the chemistry is expected to be similar. For other metals, other ligand switching reactions may also become important.

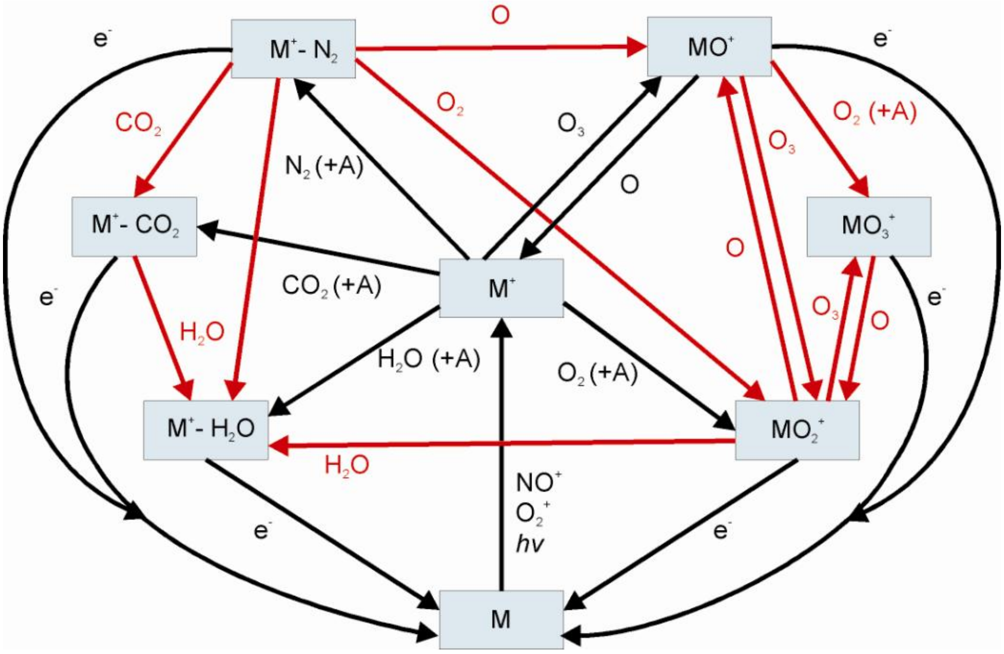

Figure 1.3. Schematic diagram summarizing the important reactions of metals in the MLT region of the atmosphere in which M= Mg^+ and Ca^+ — see text.

1.3.2 Previous work on chemistry of the metals in the MLT region of the atmosphere

In recent studies on Na[48] and K[49] high level *ab initio* calculations have been used to determine the total energies, harmonic vibrational frequencies and rotational constants of the M^+-X and the intermediate Y-M^+-X complexes in the ligand exchange reactions important in the MLT region of the upper atmosphere. The calculated values were required to calculate the corresponding rate constants through Rice-Ramsperger-Kassel-Marcus (RRKM) theory. These rate constants enable rate co-efficients measured under laboratory conditions to be extrapolated to the very low pressures of the MLT ($<10^{-5}$ bar) allowing these to be incorporated into atmospheric models to predict the vertical profiles of M containing ions against neutralization.

In one such study, the behaviour of descending E_s clouds under a range of conditions were simulated. An atmospheric model was used to model the ion-molecule chemistry of Na^+ in the simulated E_s, and hence, the correlation between the observed and predicted Na_s layers was obtained.[42] Figure 1.4 shows the comparison of the predicted and measured density profiles for Na and the descending E_s for one of the sporadic events used in reference 42.

As can be seen from Figure 1.4 good agreement is obtained between the predicted and observed time and altitude at which Na is produced from the descending E_s layer. A similar agreement was found for five out of the six cases studied and it was concluded in that investigation that ion-molecule chemistry in E_s is probably the major mechanism for producing Na_s at low- and mid-latitudes. However, the study did not rule out the possibility of other mechanisms operating, since studies have shown a strong correlation between Na_s and wind shears[50] which in some cases were in the absence of an accompanying plasma layer.[51]

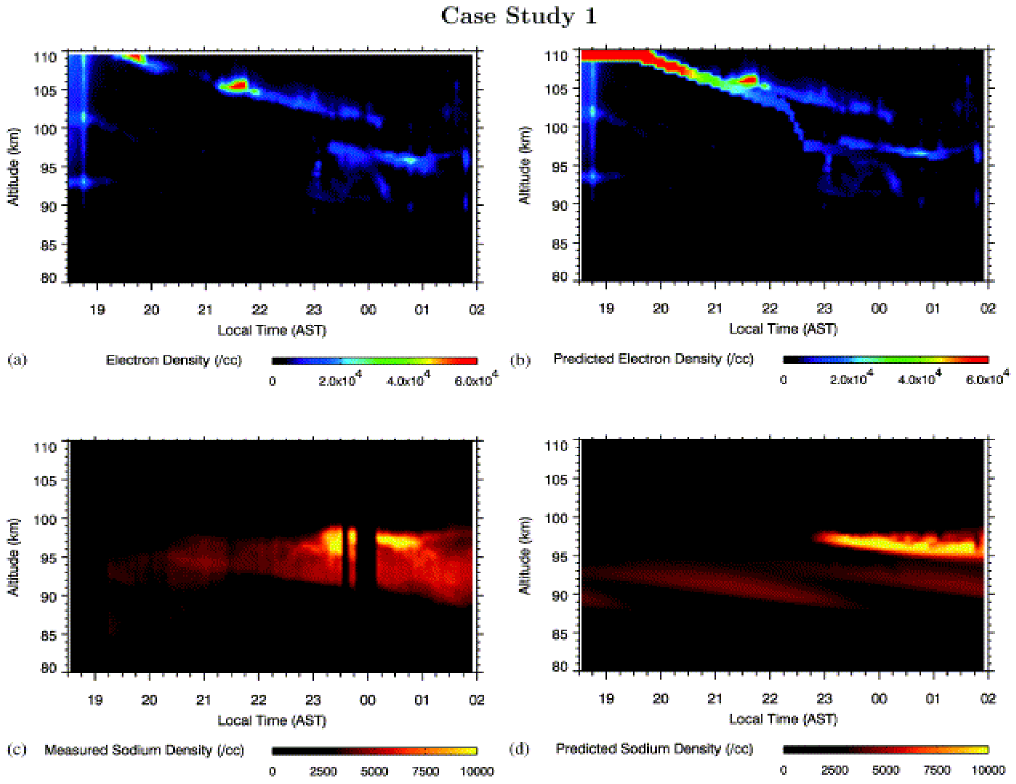

Figure 1.4. The density profile of an observed (a) descending E_s that leads to the formation of Na_s layer (c). The descent of the E_s was simulated (b) so that the Na density predicted to arise from this event by the atmospheric model (d) could be compared to that observed in the actual sporadic event.[52]

Similar studies, to that performed on the neutralisation of Na^+ have been carried out on Fe^+,[53,54] and K^+.[49] For instance, in contrast to Na^+,[48] studies on K^+ showed that it does not form strongly bound clusters with N_2, O_2 or O, unlike other metallic ions occurring in the MLT region that have been studied in the laboratory (e.g. Fe^+,[53,54] Mg^+,[55] Na^+,[47,56] Ca^+ [57]). This results in longer lifetimes of K^+ against neutralisation in comparison to the other metallic species owing to K^+ cluster lifetimes being too short to allow ligand switching reactions to form K^+-CO_2 or K^+-H_2O complexes, which can subsequently undergo dissociative recombination with electrons. An interesting point that emerges from these previous studies is that there are different dominant factors that govern the lifetimes of the various metallic ions. Whereas Na^+ is largely governed by [O][48] and Fe^+ by both [O] and [e^-],[53,54] the lifetime of K^+ is not only dependant on [O] and [e^-] but also on the local temperature.[49] This means that unless a sporadic E layer is descending into a cold region, for instance as might be produced by a gravity wave, it is unlikely that K_s layers will appear together with Na_s and Fe_s layers.

1.3.3 Present work on the chemistry of metal cations in the MLT region of the atmosphere

Magnesium is one of the most abundant metals in the MLT region with an estimated six tons being introduced in to the Earth's atmosphere each day through the ablation of meteorites. The aim of the present study is to produce data that will enable the modelling of the ion-molecule chemistry of magnesium and calcium in a similar manner to that done for Na^+ and K^+. As in previous work, the initial step is determining the dissociation energies, harmonic vibrational frequencies and rotational constants of the M^+–X and Y–M^+–X intermediate complexes that enable rate constants to be determined through RRKM theory. These RRKM calculations will be performed by Professor John Plane at the University of Leeds.

The amount of calcium present the upper atmosphere is considerably lower than that of magnesium, however, Ca^+ is unusual for a meteoric metal ion in that it can be observed by LIDAR (light detecting and ranging). This is not possible for other metals including Mg as their resonance transitions are in the UV, well below 300 nm, and are absorbed by the Huggins and Hartley bands of ozone. The chemistry of Ca^+ may be similar to that of Mg^+ and it is thought it could be used to study sporadic E_s layers. The modelling of the ion-molecule chemistry of calcium could be particularly useful in further understanding the formation of M_s from E_s in the MLT region as it allows a comparison to Ca^+ and Ca simultaneously observed through LIDAR.

References

---

[1] M. A. Duncan, *Annu. Rev. Phys. Chem.*, 1997, **48**, 69.

[2] D. Bellert and W. H. Breckenridge, *Chem. Rev.*, 2002, **102**, 1595.

[3] A. M. Knight, A. Stangassinger and M. A. Duncan, *Chem. Phys. Lett.,* 1997 **273**, 265.

[4] F. Wallimann, Dissertation *Laserspektroskopie von Metall-Edelgas-Clustern*, Phil.-nat. Fakultät, Universität Bern, 1997.

[5] W. H. Breckenridge, V. L. Ayles and T. G. Wright, *J. Phys. Chem. A*, 2008, **112**, 4209.

[6] F. Cargnoni, T. Klus, M. Mellor and R. J. Bartlet, *J. Chem. Phys.*, 2008, **129** (20), 204307.

[7] L. Xinying, C. Xue and Z. Yongfang, *Theor. Chem. Acc.*, 2009, **123**(5-6), 469.

[8] X.-F.Tong, C.-L. Yang, Y.-P. An, M.-S.Wang, X.-G. Ma and D.-H.Wang *J.*

Chem. Phys., 2009, **131**, 244304.

[9] L. R. Brock and M. A. Duncan, *J. Chem. Phys.,* 1995, **103**, 9200.

[10] L. R. Brock and M. A. Duncan, *Chem. Phys. Lett.,* 1995, **247**, 18.

[11] C. Jouvet, C. Larduex-Dedonder, S. Martrenchard and D. Solgadi, *J. Chem. Phys.,* 1991, **94**, 1759.

[12] C. S. Yeh, K. F. Whiley, D. L. Robbins and M. A. Duncan, *Int. J. Mass Spectrom. Ion Process.*, 1994, **131**, 307.

[13] C. Crépin-Gilbert and A. Tramer, *Int. Rev. Phys. Chem.*, 1999, **18**, 485.

[14] W. H. Breckenridge, V. L. Ayles and T. G. Wright, *Chem. Phys.,* 2007, **333**, 77.

[15] Y. Shen and J. J. Belbruno, *J. Phys. Chem. A.*, 2005, **109**, 10077.

[16] N. C. Bera, I. Bhattacharyya and A. K. Das, *Spectrochimica Acta A: Molecular and Biomolecular Spectroscopy,* 2007, **67**(3-4), 894.

[17] X. Li, X. Cao, J. H. Jiang and Y. F. Zhao, *Euro. Phys. J. D,* 2009, **55**(1), 87.

[18] W. H. Breckenridge, V. L. Ayles and T. G. Wright, *J. Phys. Chem. A*, 2008, **112**, 4209.

[19] A. W. K. Leung, D. Bellert, R. R. Julian and W. H. Breckenridge, *J. Chem. Phys*, 1999, **110**, 6298.

[20] K. L. Burns, D. Bellert, A. W. K. Leung and W. H. Breckenridge, *J. Chem. Phys*, 2001, **114**, 2996.

[21] P. Pyykkö, *J. Am. Chem. Soc.*, 1995, **117**, 2067.

[22] D. Schröder, H. Schwarz, J. Hrusák and P. Pyykkö, *Inorg. Chem.*, 1998, **37**, 624.

[23] http://physics.nist.gov/PhysRefData/Handbook/Tables/coppertable5.htm

---

[24] http://physics.nist.gov/PhysRefData/Handbook/Tables/silvertable5.htm

[25] http://physics.nist.gov/PhysRefData/Handbook/Tables/goldtable5.htm

[26] A. M. Gardner, R. J. Plowright, M. J. Watkins, T. G. Wright and W. H. Breckenridge, *J. Chem. Phys.*, submitted.

[27] T. G. Kane, C. S. Gardner, *Science*, 1993, **259**, 1297

[28] M. Gerding, M. Alpers, U. Von Zahn, R. J. Rollason and J. M. C. Plane, *J. Geophys. Res.*, 2000, **105**, 27131.

[29] W. J. McNeil, S. T. Lai and E. Murad, *J. Geophys. Res.*, 1998, **103**, 10899.

[30] V. M. Slipher, *Publications of the Astronomical Society of the Pacific*, 1929, **41**, 262.

[31] C. S. Gardner and M. J. Taylor, *J. Geophys. Res., 1998,* **103**, 6427.

[32] A. H. Manson, C. E. Meek, J. Qian and C. S. Gardner, *J. Geophys. Res., 1998,* **103**, 6455.

[33] R. J. States and C. S. Gardner, *J.* Atmos. Sci., 2000, **57**, 66.

[34] V. Eska, J. Hoffner and U. Von Zahn, *J. Geophys. Res., 1998,* **103**, 29207.

[35] J. M. C. Plane, *Chem. Rev.*, 2003, **103**, 4963-4984.

[36] G. E. Thomas, *J. Atmos. Terr. Phys.*, 1996, **58**, 1629.

[37] E. Murad and I. W. Williams*; Meteors in the Earth's Atmosphere,* Cambridge University Press, Cambridge, 2002

[38] T. J.Beatty, R. L. Collins, C. S. Gardener, C. A. Hostetler, C. F Sechrist and C. A. Tipley, *Geophys. Res. Lett.*, 1989, **16**, 1019.

[39] U. von Zahn and T. L. Hansen, *J. Atmos. Terr. Phys.*, 1988, **50**, 93.

[40] B. R. Clemesha, *J. Atmos. Terr. Phys.,* 1995, **57**, 725.

[41] M. Alpers, J. Hoffner and U. von Zahn, *J. Geophys. Res.,* 1994*,* **99**, 14971.

---

[42] S. C Collins, J. M. C Plane, M. C. Kelley, T. G. Wright, P. Soldan T. J. Kane, A. J. Gerrard, B. W. Grime, R. J. Rollason, J. S. Friedman, S. A. Gonzalez, Q. H. Zhou, M. P Sulzer and C. A. Tepley, *J. Atmos. Sol.-Terr. Phys.*, 2002, **64**, 845.

[43] C .J. Heinselmann, J. P. Thyer and B. J. Watkins, *J. Geophys. Res. Let.* 1998, **25**, 3059.

[44] J. D. Matthews, *J. Atmos. Sol.-Terr. Phys.*, 1998, **60**, 413.

[45] M. A. Bautista, P. Romano and A. K. Pradhan, 1998. *Astrophys. J. Sup. Ser.*, **118**, 259.

[46] G. Witt, *Space Res.*, 1969, **9**, 157

[47] R. M. Cox and J. M. C. Plane, *J. Geophys. Res.*, 1998, **103**, 6349.

[48] S. E. Daire, J. M. C. Plane, S. D. Gamblin, P. Soldán, E. P. F. Lee and T. G. Wright, *J. Atmos. Sol.-Terr. Phys.,* 2002, **64**, 863.

[49] J. M. C. Plane, R. J. Plowright and T. G. Wright, *J. Phys. Chem. A*, 2006, **110**, 3093

[50] C. S. Gardner, X. Tao and G. C. Papen, *Geophys. Res. Lett.*, 1995, **22**(20), 2809.

[51] H. Miyagawa, T. Nakamura, T. Tsuda, M. Abo, C. Nagasawa, T. D. Kawahara, K. Kobayashi and T. Kitahara, A. Nomura, *Earth Planets Space*, 1999, **51**, 785.

[52] This diagram was originally published in reference 42, Copyright Elsevier 2002.

[53] J. M. C. Plane, D. E. Self, T. Vondrak and K. R. I. Woodcock, *Adv. Space Res.,* 2003, **32** (5), 699.

[54] Vondrak, T., Woodcock, K. R. I., Plane, J. M. C., *Phys. Chem. Chem. Phys.*, 2006, **8** (4), 503.

[55] R. J. Rollason and J. M. C. Plane, *Phys. Chem. Chem. Phys.*, 2001, **3**, 4733.

---

[56] R. M. Cox and J. M. C. Plane, *J. Chem. Soc., Faraday Trans,* 1997, **93**, 2619

[57] J. M. C. Plane and R. J. Rollason, *J. Chem. Phys. A*, 2001, **105**(29), 7047.